RSC Advances

PAPER

View Article Online
View Journal | View Issue

Cite this: *RSC Adv.*, 2021, **11**, 27653

Mixed-halide triphenyl methyl radicals for site-selective functionalization and polymerization†

Lisa Chen,‡[a] Mona Arnold,‡[a] Rémi Blinder,[b] Fedor Jelezko[b] and Alexander J. C. Kuehne *[ac]

Derivatives of the stable, luminescent tris-2,4,6-trichlorophenylmethyl (TTM) radical exhibit unique doublet spin properties that are of interest for applications in optoelectronics, spintronics, and energy storage. However, poor reactivity of the chloride-moieties limits the yield of functionalization and thus the accessible variety of high performance luminescent radicals. Here, we present a pathway to obtain mixed-bromide and chloride derivatives of TTM by simple Friedel–Crafts alkylation. The resulting radical compounds show higher stability and site-specific reactivity in cross-coupling reactions, due to the better leaving group character of the *para*-bromide. The mixed halide radicals give access to complex, and so far inaccessible luminescent open-shell small molecules, as well as polymers carrying the radical centers in their backbone. The new mixed-halide triphenyl methyl radicals represent a powerful building block for customized design and synthesis of stable luminescent radicals.

Received 15th June 2021
Accepted 9th August 2021

DOI: 10.1039/d1ra04638a

rsc.li/rsc-advances

Introduction

Stable, carbon-centered π-conjugated radicals represent interesting materials for redox-active systems in organic batteries, as highly efficient electroluminescent SOMO emitters with efficiencies beyond classical spin-statistics of closed-shell organic semiconductors, and in organic spintronic applications.[1–6] Halogenated triphenyl methyl radicals (or trityl radicals) represent a prominent example of such stable, carbon-centered radicals, which are easily accessible *via* Friedel–Crafts reaction of halogenated benzenes to chloroform, followed by oxidation yielding the radical.[7,8] This reaction provides facile access to one of the few classes of luminescent open-shell molecules.[9,10] While homo-halogenated tris(perfluorophenyl) (TFM), tris(trichlorophenyl) (TTM), and tris(tribromophenyl) methyl radicals (TTBrM) have all been presented, mixed-halide radicals have not been accessible *via* the Friedel–Crafts route.[11–13] Such mixed-halide trityl methyl radicals would be of interest because *para*-bromo sites of the phenyl rings can participate in transition metal-mediated cross-coupling reactions, such as Suzuki coupling, while the halides in *ortho*-position to the central methine carbon are sterically hindered and do not take part in such functionalization. Also, TTBrM is believed to be more stable than the lighter halide homologues TTM and TFM, due to the larger size of the bromide groups and their associated steric shielding.[14] Functionalization of individual phenyl rings in all-chloro TTM has also been reported, yielding highly emissive products with significantly enhanced stability.[15,16] However, the functionalization is not selective and the yield of these products is low. By contrast, mixed-halide triphenyl methyl radicals would enable site-selective functionalization or even polymerization, thus rendering the possibility to synthesize customized open-shell molecules with unexplored properties.

Here, we report such mixed trichlorophenyl-tribromophenyl methyl radicals. We compare their optical properties as well as their stability to symmetric TTM and TTBrM systems. Furthermore, we show that our mixed halide precursors can be functionalized selectively only on the *para*-bromo position with much higher yields than in the previously pursued serendipitous functionalization. Finally we show, that the bis(tribromophenyl) (trichlorophenyl) methyl motif can be used to produce polymers with the radical in the backbone.

Results and discussion

Synthesis of mixed-halide triphenyl methyl radicals

Typically, TTM and TTBrM are prepared in bulk in a single Friedel–Crafts reaction of chloroform with trichlorobenzene or tribromobenzene followed by deprotonation and oxidation with *p*-chloranil to form the respective radical.[12,17] By contrast, our open-shell mixed halide homologues are prepared by two consecutive Friedel–Crafts reactions (see Fig. 1). The radical is produced by reaction with Bu_4NOH and *p*-chloranil.

[a]*Institute of Organic and Macromolecular Chemistry, Ulm University, Albert-Einstein-Allee 11, 89081 Ulm, Germany. E-mail: alexander.kuehne@uni-ulm.de*
[b]*Institute for Quantum Optics, Ulm University, Albert-Einstein-Allee 11, 89081 Ulm, Germany*
[c]*DWI – Leibniz-Institute for Interactive Materials, Forckenbeckstraße 50, 52074 Aachen, Germany*

† Electronic supplementary information (ESI) available. See DOI: 10.1039/d1ra04638a

‡ These authors contributed equally.

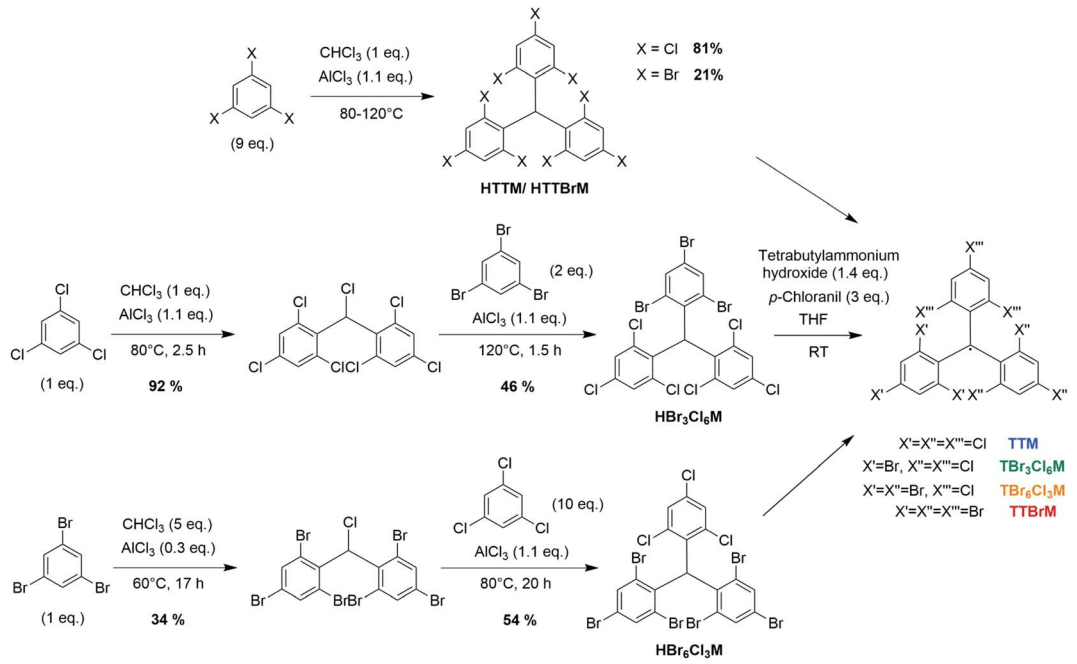

Fig. 1 Synthetic route towards mixed-halide trityl radicals using a two-step Friedel–Crafts alkylation, followed by deprotonation and subsequent oxidation. The colour code of the four different radicals in continued in the other figures.

In our synthetic strategy we first produce the homo-biphenylated product before coupling of the respective third and opposite trihalobenzene. To obtain TBr_3Cl_6M, chloroform is added stoichiometrically because once the monophenylated intermediate α,α′,2,4,6-pentachlorotoluene forms, the reactive planar benzyl carbocation immediately adds to the second trichlorobenzene, producing the desired intermediate product.[18] By contrast, to obtain the bisphenyl precursor to TBr_6Cl_3M, the larger bromo-substituents entail a higher rotation barrier in 1,3,5-tribromo-2-(dichloromethyl)benzene. It is important to perform this synthesis at 60 °C, below the melting point of tribromobenzene to avoid the formation of halide-exchanged byproducts.[19] Therefore, an excess of chloroform is required to obtain a liquid reaction mixture, yielding a considerable fraction of stable monophenylated side-product.[19] We obtain the bisphenylated products without coupling of a third phenyl ring by adjusting the ratio of tribromobenzene to chloroform (see Fig. 1). To obtain the respective mixed halide trityl compound, the bisphenyl precursors are purified and the third opposite trihalobenzene is added in excess to give the desired product after Friedel–Crafts alkylation.

In both synthetic routes towards the mixed halide compounds, the yield is limited by the Friedel–Crafts alkylation of tribromobenzene, giving overall yields for the closed-shell compounds of 42% for bis(tribromophenyl)trichlorophenyl methane (HBr_3Cl_6M) and 18% for tribromophenyl-bis(trichlorophenyl)methane (HBr_6Cl_3M). For comparison, we have also conducted the synthesis of the pure halides HTTM and HTTBrM following previously reported protocols, which gave yields of 81% and 21% in a single step.[12,17] Deprotonation and oxidation yield the respective open shell radicals, as confirmed by the clear electron paramagnetic resonance (EPR) signals (see Fig. 2a).

Characterization of mixed-halide triphenyl methyl radicals

To characterize the nonahalo-triphenyl methyl radicals we first conduct DFT studies on the U-B3LYP(6-31+G(d)) level and the energy diagram for the electronic ground state of TTM and mixed halide radicals is obtained (see Fig. 2b). The unrestricted treatment shows a large energy separation for α- and β-spin in the SOMO while the HDMO and the LUMO are almost identical for α- and β-spin. A comparison of these SOMO levels obtained by DFT with the empirically determined absorption energies obtained from UV-Vis spectroscopy suggests that the SOMO might be best described by averaging the energies of the α-state (occupied) and the and β-state (unoccupied) in the spin-unrestricted theoretical treatment (*cf.* dashed line in Fig. 2b and absorption spectra in Fig. 2c). According to the DFT calculations for the different molecules, there is no significant difference in the symmetry of the Frontier orbitals (see Fig. 2b for TBr_3Cl_6M and Fig. S3† for related radicals). Substitution of chlorine by bromine leads to a systematic bathochromic shift in the photoluminescence spectra of our nonahalo-trityl radicals. This shift can be explained by a decreasing HDMO-SOMO gap, evoked by increasing HDMO energies when substituting Cl by Br from TTM to TTBrM (from blue to red in Fig. 2b). To gain deeper insight into the emission behaviour of our radicals, we perform TD-DFT geometry optimization for the D_1 states, since the emission of TTM is supposed to arise from the vertical $D_1 \rightarrow D_0$ transition (first excited doublet state D_1 to doublet ground state D_0).[15,19] This transition corresponds to the SOMO to HDMO relaxation (*cf.* Fig. 2b). TD-DFT correctly predicts the red-

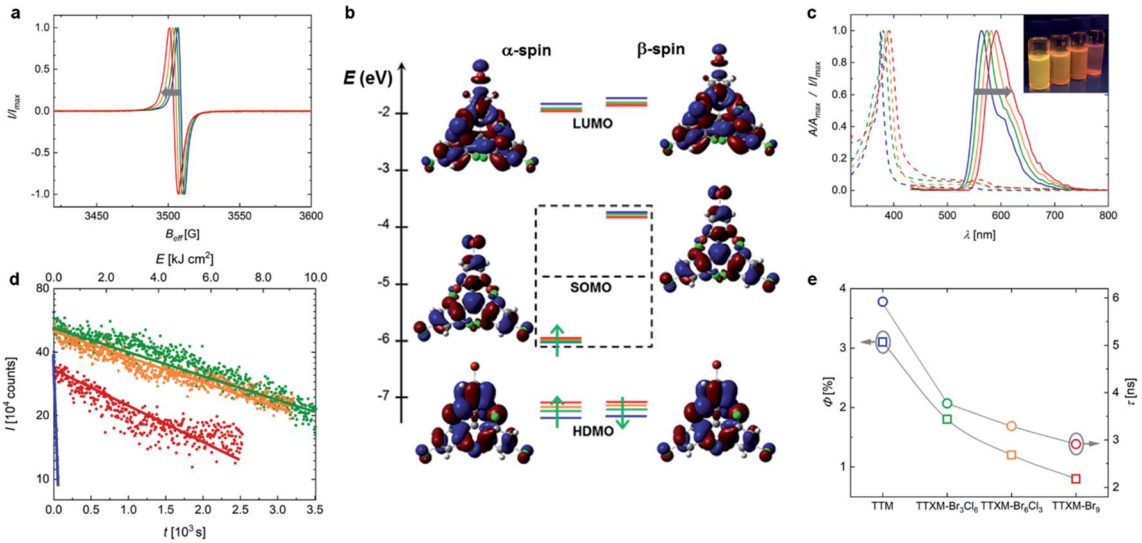

Fig. 2 (a) X-band EPR spectra of the TTM (blue), TBr_3Cl_6M (green), TBr_6Cl_3M (orange) and TTBrM (red) in toluene solution, indicating an increase of the *g*-factor with increasing number of bromine atoms. (b) Energy diagram for the electronic ground state of TTM, TBr_3Cl_6M, TBr_6Cl_3M and TTBrM radicals obtained by DFT calculations using U-B3LYP/6-31+G(d). The SOMO energies of all molecules (dashed line) are estimated by $E_{SOMO} = 1/2(E_\alpha + E_\beta)$. The Frontier orbitals are shown for the case of TBr_3Cl_6M. (c) Absorption (dashed line) and photoluminescence (solid line) spectra of TTXM radicals. The emission is bathochromically shifted from yellow to red with increasing number of bromine atoms. The inset shows a photograph of solutions of TTM, TBr_3Cl_6M, TBr6Cl_3M and TTBrM (from left to right) in toluene under irradiation at 365 nm. (d) Fluorescence decay of TTXM in degassed toluene solutions (1 mM) under irradiation using a 355 nm pulsed laser (pulse width: 7 ns, frequency: 10 Hz, energy density: 2.87×10^5 μJ cm^{-2}). The lines are a guide to the eye. (e) Photoluminescence quantum yield (ϕ) (squares) and fluorescence lifetimes (τ) (circles) of TTXM radicals in dichloromethane solution obtained from measurements using an integrating sphere and applying transient PL measurements, respectively. The connecting lines are a guide to the eye. Both values decrease with increasing number of bromine atoms.

shift observed in our empirical photoluminescence experiment (see Table S1†). Furthermore, we observe increasing *g*-factors of the unpaired electron in our EPR experiment for increasing degrees of bromo-functionalization, indicating stronger spin–orbit interactions of the heavier bromine atoms (see Fig. 2a).[20] The introduction of brominated phenyl rings also increases the stability of the radicals against photo-bleaching (see Fig. 2d). The improved fastness derives presumably from enhanced spin–orbit coupling together with the enhanced steric hindrance with increasing bromine-functionalization, thus preventing rotation and offering better protection of the radical centre from oxidation and intramolecular ring-closing reactions. However, advancing substitution of chlorides by bromides leads to decreasing photoluminescence quantum yields (ϕ) from 3.1% for TTM to 0.8% for TTBrM – ϕ of the mixed halide radicals are between these values. In addition, the fluorescence lifetime (τ) is reduced from 5.9 ns for TTM to 2.9 ns for TTBrM – again, the mixed halide radicals exhibit fluorescence lifetimes inside of this interval (see Fig. 2e and S4†). The rate constants of radiative (k_r) and non-radiative decay (k_{nr}), can be estimated from ϕ and τ using the following equations:

$$\phi = \frac{k_r}{k_r + k_{nr}}$$

$$\tau = \frac{1}{k_r + k_{nr}}$$

k_{nr} rises with an increasing number of bromine atoms, while k_r decreases (see Table 1). Previously, this phenomenon has been explained by a more planar conformation of the phenyl rings and stronger electron delocalization for lighter halo-atoms. The enhanced π-conjugation facilitates fluorescence by significantly suppressing vibrational relaxation.[14] Conversely, the heavier

Table 1 Photophysical and EPR properties of mixed halide TTMs

Compound	*g*-Factor[a] [–]	Φ[b] [%]	τ[c] [ns]	k_r[d] [10^6 s^{-1}]	k_{nr}[d] [10^6 s^{-1}]	$t_{1/2}$[e] [10^3 s]	$E_{1/2}$[e] [kJ cm^2]
TTM	2.0037	3.1	5.92	5.24	163.68	0.01	0.03
TBr_3Cl_6M	2.0045	1.8	3.77	4.77	260.48	2.40	7.08
TBr_6Cl_3M	2.0056	1.2	3.29	3.64	300.30	2.31	6.51
TTBrM	2.0066	0.8	2.91	2.75	340.89	1.70	4.71

[a] In toluene solution at 25 °C. [b] ϕ in DCM solution. [c] In oxygen-free DCM at 25 °C. [d] Rate constants calculated using $\phi = k_r/(k_r + k_{nr})$ and $\tau = 1/(k_r + k_{nr})$. [e] In 1 mM oxygen-free toluene irradiated at 355 nm (energy density: 2.87×10^5 μJ cm^{-2}, pulse width: 7 ns, frequency: 10 Hz).

bromine atoms in our mixed halide radicals prevent a co-planar conformation of the molecules, thus assisting non-radiative vibrational relaxation, causing the reduction in ϕ with increasing bromine content.

Cross-coupling reactions of mixed-halide triphenyl methanes as radical precursors for small molecules

To showcase the usefulness of our mixed halide radicals, we perform transition metal catalysed cross-coupling reactions, which preferentially involve the *para*-bromide-functionality due to their better leaving-group character *versus* the chloride-sites.[21] This will give access to radicals of anisotropic and complex structure that have been inaccessible to date. We test our mixed-halide compounds in a variety of transition metal medicated C–C cross-coupling reactions (see Table S3†). While cross-coupling under typical Heck-, direct arylation-, and Yamamoto-reaction conditions are challenging, the mixed-halide molecules successfully undergo Suzuki-, Sonogashira- and Stille-type coupling reactions. Coupling to HBr_3Cl_6M followed by deprotonation and oxidation yields monofunctional radicals or bridged biradicals (see Fig. 3a and S5a,c†). By coupling two phenylacetylene molecules to HBr_6Cl_3M and subsequent conversion to the radical, a bi-functionalized open-shell molecule is obtained (see Fig. S5b†). Single peaks in the EPR spectra indicate successful conversion and that the unpaired electron of these species is localized at the central methine atom (see Fig. S6†). UV-Vis absorption spectroscopy reveals a strong band for all radical species at ~400 nm, which is absent in the respective closed-shell precursors (*cf.* red and grey dashed lines in Fig. 3a and S5†). Concomitantly, the emission of the open-shell molecules exhibits a bathochromic shift to the red spectrum around 600 nm, compared to the corresponding closed-shell molecules (see Fig. 3a and S5a–c†). Note that we observe partial substitution of the *ortho*-bromines with hydrogens during Suzuki-coupling (see ^{1}H-NMR spectra in ESI†). We hypothesize that after successful coupling of the boronic acid compound to the bromine atoms in *para*-position, the bromides in *ortho*-position to the central methine group are attacked by the palladium catalyst. Due to steric hindrance, coupling with another boronic acid compound is prevented, leading to dehalogenation *via* β-hydride elimination as a side reaction.[22] However, the resulting radicals appear relatively stable and exhibit EPR signals after weeks of storage despite the dehalogenation (see Fig. S6d†). To date, almost exclusively electron donor groups have been coupled to TTM. Coupling of an acceptor unit to the TTM radical moiety would endow this open-shell molecule with new electronic and emissive properties.[2] The pyrimidine-functionalization of the TBr_3Cl_6M represents such an acceptor-coupled radical, emphasizing the huge potential of our synthetic approach for the design of organic luminescent radicals of novel electronic structure (see Fig. 3a).[2]

Radical polymers obtained by cross-coupling reactions of mixed-halide triphenyl methanes

To highlight the full potential of our selectively addressable trityl units, we also employ HBr_6Cl_3M in Stille-, Sonogashira-, and Suzuki-polymerizations. Successful coupling is confirmed by ^{1}H-NMR, size exclusion chromatography (SEC), and MALDI-ToF (the latter only for the Sonogashira coupled polyradical). MALDI-ToF clearly shows the repeating unit of the polyradical (see ESI for NMR spectra and Fig. S2†). The resulting polymers exhibit M_w of 14–17 kDa as determined by SEC. The polymers can be converted into the open-shell species by deprotonation and subsequent oxidation, yielding linear polymers with the radical moieties as part of the backbone, as confirmed by EPR spectroscopy (see Fig. S6e†). The synthesis of such conjugated polymers with radical electrons in their backbone is unprecedented. However, spin-density measurements indicate that the conversion to the open-shell trityl radical is incomplete at 2–3% (and up to 25% for poly(fluorene-*co*-TBr_6Cl_3M) obtained by Suzuki coupling) when applying standard reaction conditions. This low yield in conversion to the radical species could originate either from (i) inefficient deprotonation and oxidation or (ii) radical electron combination after oxidation, producing quinodal π-conjugation along the backbone. Since radicals as well as quinodal structures are NMR silent, we turn to IR- and Raman-spectroscopy but we do not detect a difference between the precursor and the polymer converted to the radical (see Fig. S7†). However, when we employ higher temperature and larger concentrations of base, we observe higher degrees of conversion up to 40% (see Table S4†). The absorption spectra of the radical polymers resemble those of the closed-shell precursor polymers; however, with an additional absorption band at lower energies, originating from the HDMO–SOMO

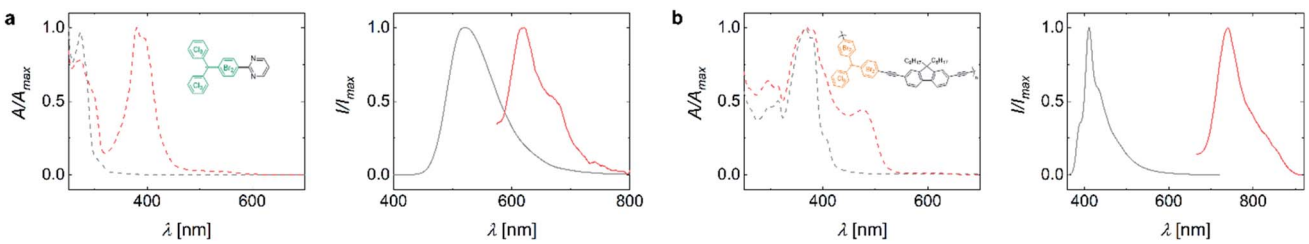

Fig. 3 Normalized absorption (dashed lines) and photoluminescence spectra (solid lines) of (a) a pyrimidine-functionalized radical and (b) a polymer radical (red) in dichloromethane. The spectra of their precursors (grey) in the same solvent are shown for comparison. The photoluminescence spectra of the radicals result from excitation at the wavelength of the HDMO to SOMO transition.

transition as in the case of the small molecular radicals. When exciting the polymers into this absorption band, we observe deep red emission of low intensity (*cf.* grey and red curves in Fig. 3b and S5d, e†).

Conclusions

The simple functionalization of our mixed-halide compounds gives access to fine-tuning and tailoring of the properties of TTM-type radicals and the paradigm of more complex open-shell molecules. Especially the successful synthesis of polymers with radical centres in the backbone, as a first of its kind, showcases the manifold possibilities of designing future unprecedented open-shell molecules. This facile functionalization of open-shell molecules provides great potential for new applications of radical emitters. Such novel open-shell compounds will find application as luminophores in optoelectronics, as spin-sensitive sensors in the field of spintronics, or as active electrode material.

Experimental section

Materials

All reagents and solvents are purchased from Sigma-Aldrich, TCI chemicals or Alfa Aesar and are used without further purification. All reactions are performed under argon atmosphere.

General methods

NMR spectroscopy. The ^{1}H and ^{13}C NMR spectra are recorded on a 400 MHz Bruker Avance DRX 400 spectrometer. The chemical shifts (δ) in the ^{1}H-NMR spectra are reported in parts per million (ppm) *versus* the residual proton content of the deuterated solvent at ambient temperature, coupling constants are given in Hertz (Hz). The spin multiplicities are designated as follows: s = singlet, d = doublet, t = triplet and m = multiplet. The obtained data are evaluated with the MestReNova program from Mestrelab Research.

MALDI-ToF mass spectrometry. MALDI-FTICR spectra of the small organic molecules are recorded on a solariX mass spectrometer (Bruker Daltonics) using *trans*-2-[3-(4-*t*-butyl-phenyl)-2-methyl-2-propenylidene]malononitrile (DCTB) as matrix. The polymer samples are analyzed by MALDI-ToF mass spectrometry using a solvent-free sample preparation method. The matrix (DCTB) and the polymer are mixed with a Retsch MM400 ball mill for 30 min (frequency: 30 Hz) and the resulting powder is applied on the MALDI target plate. The spectra are recorded on a Bruker rapifleX mass spectrometer in the linear mode.

UV-Vis spectroscopy. UV-Vis measurements are performed using a Lambda 365 spectrophotometer by Perkin Elmer with UV WinLab as standard software. The measurements are carried out within the wavelength range of 250–800 nm with a scan speed of 600 nm min^{-1}. The samples are diluted in toluene as standard solvent and measured in 1 cm quartz glass cuvettes.

Photoluminescence spectroscopy. The fluorescence spectra of the precursor components are recorded with a PerkinElmer FL6500 within a wavelength range of 350–800 nm. Quantum yields of the radicals in dichloromethane are measured with the same spectrometer equipped with an integrating sphere. Fluorescence spectra of the radicals are recorded on a custom build laser reflection spectrometer from AIQTEC that is described in detail below.

EPR spectroscopy. Electron Paramagnetic Resonance spectra are recorded using a X-band EPR system (Bruker ELEXSYS E580) with an ER 4122 SHQE cavity, using the software xEPR for data acquisition. Measurements are performed at microwave frequency $f_X \approx 9.84$ GHz, with a resonance quality factor $Q = 8000$, a power 0.15 mW (30 dB attenuation in xEPR). Modulation amplitude and frequencies are 1 G/100 kHz. Prior to the measurement, samples are inserted into 4 mm quartz EPR tubes (Wilmad 707-SQ-100M) and dissolved into toluene. The acquisition time for each spectrum is 40 s. For better illustration the magnetic field of all four compounds is normalized considering the microwave frequency used for the measurement on TBr_3Cl_6M. Determination of the radical concentration was performed using the built-in spin-counting module, available in xEPR.

Infrared spectroscopy. The infrared spectra are either collected on a PerkinElmer Spectrum two spectrometer or on a Bruker Alpha II spectrometer, both equipped with a diamond ATR-crystal.

Gel permeation chromatography (GPC). The molecular weight of the polymer is determined by gel permeation chromatography (GPC) on a 1260 Infinity II GPC/SEC System from Agilent Technologies with polystyrene as a standard and THF as the eluent.

Photostability measurement. Photostability experiments are performed on an AIQTEC Microscopic Imaging Spectrometer (MIS1000). Prior to measurement the sample is dissolved in toluene (2 mM) and purged with argon in a sealable 1 cm quartz glass cuvette. The cuvette is placed on an inverted microscope equipped with a 40× objective. The laser source is a frequency-tripled Nd:YAG laser with a pulse duration of 7 ns at a repetition rate of 10 Hz. For the photostability studies the sample is exposed to the pulsed laser with an energy density of 2.87×10^5 μJ cm^{-2} over a certain time period. Photoluminescence and reflected light are collected through the same former mentioned objective and sent through a spectral edgepass filter (cut-on wavelength 400 nm) to filter out the excitation signal. The filtered signal is then sent through a spectrograph with an ICCD sensor to collect the emission spectra after each laser pulse. The intensity profiles in the studies are obtained by integration of the emission spectra and evaluation over time.

Time-correlated single-photon counting (TCPSC). The fluorescence lifetime measurements are also conducted on the MIS 1000, which is also equipped with a fs-pulsed laser diode with an emission wavelength at 375 nm and a repetition rate of 80 MHz. The samples are measured under argon atmosphere in a sealed cuvette, which is placed on top of the objective with 40× magnification. The signal is detected by a TCSPC photodiode attached to the spectrometer. The grating of the spectrometer is centered at the wanted detection wavelength and the slit of the spectrometer is set at 100 μm.

DFT/TD-DFT. DFT and TD-DFT calculations are performed on the TTXM radicals with Gaussian g16.C.01.[23] The exchange-correlation functional UB3LYP of Becke, Lee, Yang and Parr is applied with the 6-31+G(d) basis set.[24–28] Diffuse functions and additional polarization functions are important for the heavy atoms, while both functions on hydrogen atoms do not lead to significant changes. The structures of the radicals are optimized geometrically *in vacuo*. Molecular orbitals are visualized with Gaussview 6.1.[29] The electronic self-consistent field (SCF) procedure is considered to be converged when the total energy difference is less than 10^{-4} eV, and all forces are at least smaller than 10^{-5} eV Å^{-1}.

Author contributions

AJCK devised the project. AJCK, LC, and MA designed the study, and MA and LC synthesized and characterized the compounds. LC performed transient spectroscopy, MA performed quantum chemical calculations. RB and FJ provided support for the EPR experiments. AJCK, LC, and MA wrote the paper, all authors discussed and commented on the manuscript.

Conflicts of interest

There are no conflicts to declare.

Acknowledgements

The authors gratefully acknowledge fruitful discussions with F. Deschler (TUM, Germany). The authors also thank Dr Hans-Joachim Räder from the Max-Planck-Institute for Polymer Research for performing MALDI-ToF measurements of the polymers and Dr Markus Lamla at Uni Ulm for performing MALDI-FTICR measurements of the small organic molecules. The German research foundation is acknowledged for funding within the priority program SPP 2248 Polymer-Based Batteries.

Notes and references

1 Q. Peng, A. Obolda, M. Zhang and F. Li, *Angew. Chem., Int. Ed.*, 2015, **54**, 7091–7095.
2 Y. Gao, W. Xu, H. Ma, A. Obolda, W. Yan, S. Dong, M. Zhang and F. Li, *Chem. Mater.*, 2017, **29**, 6733–6739.
3 X. Ai, E. W. Evans, S. Dong, A. J. Gillett, H. Guo, Y. Chen, T. J. H. Hele, R. H. Friend and F. Li, *Nature*, 2018, **563**, 536–540.
4 K. Nakahara, S. Iwasa, M. Satoh, Y. Morioka, J. Iriyama, M. Suguro and E. Hasegawa, *Chem. Phys. Lett.*, 2002, **359**, 351–354.
5 L. Poggini, G. Cucinotta, L. Sorace, A. Caneschi, D. Gatteschi, R. Sessoli and M. Mannini, *Rend. Lincei*, 2018, **29**, 623–630.
6 M. Mas-Torrent, N. Crivillers, V. Mugnaini, I. Ratera, C. Rovira and J. Veciana, *J. Mater. Chem.*, 2009, **19**, 1691–1695.
7 B. Manuel, R. Juan, C. Juan, R. Concepción and A. Olag, *Synthesis*, 1986, **1**, 64–66.
8 Y. Hattori, T. Kusamoto and H. Nishihara, *Angew. Chem., Int. Ed.*, 2014, **53**, 11845–11848.
9 G. N. Lewis, D. Lifkin and T. T. Magel, *J. Am. Chem. Soc.*, 1944, **66**, 1579–1583.
10 D. T. Breslin and M. A. Fox, *J. Phys. Chem.*, 1994, **98**, 408–411.
11 C. Trapp, C. S. Wang and R. Filler, *J. Chem. Phys.*, 1966, **45**, 3470–3472.
12 O. Armet, J. Veciana, C. Rovira, J. Riera, J. Castañer, E. Molins, J. Rius, C. Miravitlles, S. Olivella and J. Brichfeus, *J. Phys. Chem.*, 1987, **91**, 5608–5616.
13 C. Liu, E. Hamzehpoor, Y. Sakai-Otsuka, T. Jadhav and D. F. Perepichka, *Angew. Chem.*, 2020, **8**, 23030–23034.
14 Y. Hattori, T. Kusamoto and H. Nishihara, *RSC Adv.*, 2015, **5**, 64802–64805.
15 H. Guo, Q. Peng, X. Chen, Q. Gu, S. Dong, E. W. Evans, A. J. Gillett, X. Ai, M. Zhang, D. Credgington, V. Coropceanu, R. H. Friend, J. Brédas and F. Li, *Nat. Mater.*, 2019, **18**, 977–984.
16 S. Castellanos, D. Velasco, F. López-Calahorra, E. Brillas and L. Julia, *J. Org. Chem.*, 2008, **73**, 3759–3767.
17 P. Mayorga-burrezo, V. G. Jiménez, D. Blasi, T. Parella, I. Ratera, A. G. Campaña and J. Veciana, *Chem.–Eur. J.*, 2020, **26**, 3776–3781.
18 B. J. Fuhr, B. W. Goodwin, H. M. Hutton and T. Schaefer, *Can. J. Chem.*, 1970, **48**, 1558–1565.
19 J. Peeling, L. Ernst and T. Schaefer, *Can. J. Chem.*, 1974, **52**, 849–854.
20 R. L. Hota and G. S. Tripathi, *J. Phys.: Condens. Matter*, 1991, **3**, 6299–6311.
21 R. Rossi, F. Bellina and M. Lessi, *Adv. Synth. Catal.*, 2012, **354**, 1181–1255.
22 Z. Ahmadi and J. S. McIndoe, *Chem. Commun.*, 2013, **49**, 11488–11490.
23 M. J. Frisch, *Gaussian*, Wallingford, CT, 2016.
24 A. D. Becke, *J. Chem. Phys.*, 1992, **96**, 2155–2160.
25 R. G. Parr, C. Lee and W. Yang, *Phys. Rev. B: Condens. Matter Mater. Phys.*, 1988, **37**, 785–789.
26 K. Kim and K. D. Jordan, *J. Phys. Chem.*, 1994, **98**, 10089–10094.
27 G. A. Petersson, A. Bennett, T. G. Tensfeldt, M. A. Al-Laham, W. A. Shirley and J. Mantzaris, *J. Chem. Phys.*, 1988, **89**, 2193–2218.
28 G. A. Petersson and M. A. Al-Laham, *J. Chem. Phys.*, 1991, **94**, 6081–6090.
29 R. Dennington and J. Millam, *GaussView, Version 6.1*, Semichem Inc., Shawnee Mission, KS, 2016.